
SUNRISE: A Simple Unified Framework for Ensemble Learning in Deep Reinforcement Learning

Kimin Lee
UC Berkeley

Michael Laskin
UC Berkeley

Aravind Srinivas
UC Berkeley

Pieter Abbeel
UC Berkeley

Abstract

Model-free deep reinforcement learning (RL) has been successful in a range of challenging domains. However, there are some remaining issues, such as stabilizing the optimization of nonlinear function approximators, preventing error propagation due to the Bellman backup in Q-learning, and efficient exploration. To mitigate these issues, we present SUNRISE, a simple unified ensemble method, which is compatible with various off-policy RL algorithms. SUNRISE integrates three key ingredients: (a) bootstrap with random initialization which improves the stability of the learning process by training a diverse ensemble of agents, (b) weighted Bellman backups, which prevent error propagation in Q-learning by reweighing sample transitions based on uncertainty estimates from the ensembles, and (c) an inference method that selects actions using highest upper-confidence bounds for efficient exploration. Our experiments show that SUNRISE significantly improves the performance of existing off-policy RL algorithms, such as Soft Actor-Critic and Rainbow DQN, for both continuous and discrete control tasks on both low-dimensional and high-dimensional environments. Our training code is available at <https://github.com/pokaxpoka/sunrise>.

1 Introduction

Model-free reinforcement learning (RL), with high-capacity function approximators, such as deep neural networks (DNNs), has been used to solve a variety of sequential decision-making problems, including board games [38, 39], video games [32, 48], and robotic manipulation [24]. It has been well established that the above successes are highly sample *inefficient* [23]. Recently, a lot of progress has been made in more sample-efficient model-free RL algorithms through improvements in off-policy learning both in discrete and continuous domains [14, 15, 20]. However, there are still substantial challenges when training off-policy RL algorithms. First, the learning process is often unstable and sensitive to hyperparameters because it is a complex problem to optimize large nonlinear policies such as DNNs [19]. Second, Q-learning often converges to sub-optimal solutions due to error propagation in the Bellman backup, i.e., the errors induced in the target value can lead to an increase in overall error in the Q-function [26, 27]. Third, it is hard to balance exploration and exploitation, which is necessary for efficient RL [10, 33] (see Section 2 for further details).

One way to address the above issues with off-policy RL algorithms is to use ensemble methods, which combine multiple models of the value function and (or) policy [10, 29, 33, 51]. One example is the twin-Q trick [14] that was proposed to handle the overestimation of value functions for continuous control tasks. Bootstrapped DQN [33] leveraged an ensemble of Q-functions for more effective exploration, and Chen et al. [10] further improved it by adapting upper-confidence bounds algorithms [3, 4] based on uncertainty estimates from ensembles. However, most prior works have studied the various axes of improvements from ensemble methods in isolation and have ignored the error propagation aspect.

In this paper, we present SUNRISE, a simple unified ensemble method that is compatible with most modern off-policy RL algorithms, such as Q-learning and actor-critic algorithms. SUNRISE consists of the following key ingredients (see Figure 1(a)):

- **Bootstrap with random initialization:** To enforce diversity between ensemble agents, we initialize the model parameters randomly and apply different training samples to each agent. Similar to Osband et al. [33], we find that this simple technique stabilizes the learning process and improves performance by combining diverse agents.
- **Weighted Bellman backup:** Errors in the target Q-function can propagate to the current Q-function [26, 27] because the Bellman backup is usually applied with a learned target Q-function (see Section 3.2 for more details). To handle this issue, we reweigh the Bellman backup based on uncertainty estimates of target Q-functions. Because prediction errors can be characterized by uncertainty estimates from ensembles (i.e., variance of predictions) as shown in Figure 1(b), we find that the proposed method significantly mitigates error propagation in Q-learning.
- **UCB exploration:** We define an upper-confidence bound (UCB) based on the mean and variance of Q-functions similar to Chen et al. [10], and introduce an inference method, which selects actions with highest UCB for efficient exploration. This inference method can encourage exploration by providing a bonus for visiting unseen state-action pairs, where ensembles produce high uncertainty, i.e., high variance (see Figure 1(b)).

We demonstrate the effectiveness of SUNRISE using Soft Actor-Critic (SAC) [15] for continuous control benchmarks (specifically, OpenAI Gym [9] and DeepMind Control Suite [43]) and Rainbow DQN [20] for discrete control benchmarks (specifically, Atari games [6]). In our experiments, SUNRISE consistently improves the performance of existing off-policy RL methods and outperforms baselines, including model-based RL methods such as POPLIN [49], Dreamer [17], and SimPLe [23].

2 Related work

Off-policy RL algorithms. Recently, various off-policy RL algorithms have provided large gains in sample-efficiency by reusing past experiences [14, 15, 20]. Rainbow DQN [20] achieved state-of-the-art performance on the Atari games [6] by combining several techniques, such as double Q-learning [46] and distributional DQN [7]. For continuous control tasks, SAC [15] achieved state-of-the-art sample-efficiency results by incorporating the maximum entropy framework, and Laskin et al. [30] showed that the sample-efficiency of SAC can be further improved on high-dimensional environments by incorporating data augmentations. Our ensemble method brings orthogonal benefits and is complementary and compatible with these existing state-of-the-art algorithms.

Ensemble methods in RL. Ensemble methods have been studied for different purposes in RL [1, 2, 10, 12, 28, 33, 51]. Chua et al. [12] showed that modeling errors in model-based RL can be reduced using an ensemble of dynamics models, and Kurutach et al. [28] accelerated policy learning by generating imagined experiences from the ensemble of dynamics models. Bootstrapped DQN [33] leveraged the ensemble of Q-functions for efficient exploration. However, our method is different in that we propose a unified framework that handles various issues in off-policy RL algorithms.

Stabilizing Q-learning. It has been empirically observed that instability in Q-learning can be caused by applying the Bellman backup on the learned value function [2, 14, 18, 26, 27, 46]. For discrete control tasks, double Q-learning [18, 46] addressed the value overestimation by maintaining two independent estimators of the action values and later extended to continuous control tasks in TD3 [14]. Recently, Kumar et al. [27] handled the error propagation issue by reweighting the Bellman backup based on cumulative Bellman errors. While most prior work has improved the stability by taking the minimum over Q-functions or estimating cumulative errors, we propose an alternative way that also utilizes ensembles to estimate uncertainty and provide more stable, higher-signal-to-noise back-ups.

Exploration in RL. To balance exploration and exploitation, several methods, such as the maximum entropy frameworks [15, 53] and exploration bonus rewards [5, 11, 21, 34], have been proposed. Despite the success of these exploration methods, a potential drawback is that agents can focus on irrelevant aspects of the environment because these methods do not depend on the rewards. To handle this issue, Chen et al. [10] proposed an exploration strategy that considers both best estimates (i.e., mean) and uncertainty (i.e., variance) of Q-functions for discrete control tasks. We further extend this strategy to continuous control tasks and show that it can be combined with other techniques.

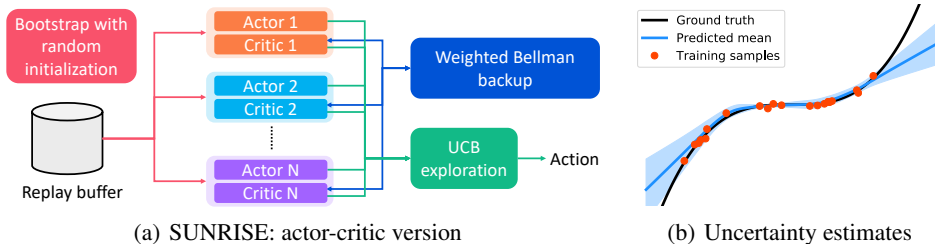


Figure 1: (a) Illustration of our framework. We consider N independent agents (i.e., no shared parameters between agents) with one replay buffer. (b) Uncertainty estimates from an ensemble of neural networks on a toy regression task (see Appendix C for more experimental details). The black line is the ground truth curve, and the red dots are training samples. The blue lines show the mean and variance of predictions over ten ensemble models. The ensemble can produce well-calibrated uncertainty estimates (i.e., variance) on unseen samples.

3 SUNRISE

We present SUNRISE: Simple UNified framework for ReInforcement learning using enSEMBles. In principle, SUNRISE can be used in conjunction with most modern off-policy RL algorithms, such as SAC [15] and Rainbow DQN [20]. For the exposition, we describe only the SAC version of SUNRISE in the main body. The Rainbow DQN version of SUNRISE follows the same principles and is fully described in Appendix B.

3.1 Preliminaries: reinforcement learning and soft actor-critic

We consider a standard RL framework where an agent interacts with an environment in discrete time. Formally, at each timestep t , the agent receives a state s_t from the environment and chooses an action a_t based on its policy π . The environment returns a reward r_t and the agent transitions to the next state s_{t+1} . The return $R_t = \sum_{k=0}^{\infty} \gamma^k r_{t+k}$ is the total accumulated rewards from timestep t with a discount factor $\gamma \in [0, 1)$. RL then maximizes the expected return from each state s_t .

SAC [15] is an off-policy actor-critic method based on the maximum entropy RL framework [53], which encourages the robustness to noise and exploration by maximizing a weighted objective of the reward and the policy entropy (see Appendix A for further details). To update the parameters, SAC alternates between a soft policy evaluation and a soft policy improvement. At the soft policy evaluation step, a soft Q-function, which is modeled as a neural network with parameters θ , is updated by minimizing the following soft Bellman residual:

$$\mathcal{L}_{\text{critic}}^{\text{SAC}}(\theta) = \mathbb{E}_{\tau_t \sim \mathcal{B}}[\mathcal{L}_Q(\tau_t, \theta)], \quad (1)$$

$$\mathcal{L}_Q(\tau_t, \theta) = (Q_\theta(s_t, a_t) - r_t - \gamma \mathbb{E}_{a_{t+1} \sim \pi_\phi} [Q_{\bar{\theta}}(s_{t+1}, a_{t+1}) - \alpha \log \pi_\phi(a_{t+1}|s_{t+1})])^2, \quad (2)$$

where $\tau_t = (s_t, a_t, r_t, s_{t+1})$ is a transition, \mathcal{B} is a replay buffer, $\bar{\theta}$ are the delayed parameters, and α is a temperature parameter. At the soft policy improvement step, the policy π with its parameter ϕ is updated by minimizing the following objective:

$$\mathcal{L}_{\text{actor}}^{\text{SAC}}(\phi) = \mathbb{E}_{s_t \sim \mathcal{B}}[\mathcal{L}_\pi(s_t, \phi)], \text{ where } \mathcal{L}_\pi(s_t, \phi) = \mathbb{E}_{a_t \sim \pi_\phi} [\alpha \log \pi_\phi(a_t|s_t) - Q_\theta(s_t, a_t)]. \quad (3)$$

Here, the policy is modeled as a Gaussian with mean and covariance given by neural networks to handle continuous action spaces.

3.2 Unified ensemble methods for off-policy RL algorithms

In the design of SUNRISE, we integrate the three key ingredients, i.e., bootstrap with random initialization, weighted Bellman backup, and UCB exploration, into a single framework.

Bootstrap with random initialization. Formally, we consider an ensemble of N SAC agents, i.e., $\{Q_{\theta_i}, \pi_{\phi_i}\}_{i=1}^N$, where θ_i and ϕ_i denote the parameters of the i -th soft Q-function and policy.¹ To

¹We remark that each Q-function $Q_{\theta_i}(s, a)$ has a unique target Q-function $Q_{\bar{\theta}_i}(s, a)$.

Algorithm 1 SUNRISE: SAC version

```
1: for each iteration do
2:   for each timestep  $t$  do
3:     // UCB EXPLORATION
4:     Collect  $N$  action samples:  $\mathcal{A}_t = \{a_{t,i} \sim \pi_{\phi_i}(a|s_t) | i \in \{1, \dots, N\}\}$ 
5:     Choose the action that maximizes UCB:  $a_t = \operatorname{argmax}_{a_{t,i} \in \mathcal{A}_t} Q_{\text{mean}}(s_t, a_{t,i}) + \lambda Q_{\text{std}}(s_t, a_{t,i})$ 
6:     Collect state  $s_{t+1}$  and reward  $r_t$  from the environment by taking action  $a_t$ 
7:     Sample bootstrap masks  $M_t = \{m_{t,i} \sim \text{Bernoulli}(\beta) | i \in \{1, \dots, N\}\}$ 
8:     Store transitions  $\tau_t = (s_t, a_t, s_{t+1}, r_t)$  and masks in replay buffer  $\mathcal{B} \leftarrow \mathcal{B} \cup \{(\tau_t, M_t)\}$ 
9:   end for
10:  // UPDATE AGENTS VIA BOOTSTRAP AND WEIGHTED BELLMAN BACKUP
11:  for each gradient step do
12:    Sample random minibatch  $\{(\tau_j, M_j)\}_{j=1}^B \sim \mathcal{B}$ 
13:    for each agent  $i$  do
14:      Update the Q-function by minimizing  $\frac{1}{B} \sum_{j=1}^B m_{j,i} \mathcal{L}_{WQ}(\tau_j, \theta_i)$ 
15:      Update the policy by minimizing  $\frac{1}{B} \sum_{j=1}^B m_{j,i} \mathcal{L}_{\pi}(s_j, \phi_i)$ 
16:    end for
17:  end for
18: end for
```

train the ensemble of agents, we use the bootstrap with random initialization [13, 33], which enforces the diversity between agents through two simple ideas: First, we initialize the model parameters of all agents with random parameter values for inducing an initial diversity in the models. Second, we apply different samples to train each agent. Specifically, for each SAC agent i in each timestep t , we draw the binary masks $m_{t,i}$ from the Bernoulli distribution with parameter $\beta \in (0, 1]$, and store them in the replay buffer. Then, when updating the model parameters of agents, we multiply the bootstrap mask to each objective function, such as: $m_{t,i} \mathcal{L}_Q(\tau_t, \theta_i)$ and $m_{t,i} \mathcal{L}_{\pi}(s_t, \phi_i)$ in (2) and (3). We remark that Osband et al. [33] applied this simple technique to train an ensemble of DQN [32] only for discrete control tasks, while we apply to SAC [15] and Rainbow DQN [20] for both continuous and discrete tasks with additional techniques in the following paragraphs.

Weighted Bellman backup. Since conventional Q-learning is based on the Bellman backup in (2), it can be affected by error propagation. I.e., error in the target Q-function $Q_{\bar{\theta}}(s_{t+1}, a_{t+1})$ gets propagated into the Q-function $Q_{\theta}(s_t, a_t)$ at the current state. Recently, Kumar et al. [27] showed that this error propagation can cause inconsistency and unstable convergence. To mitigate this issue, for each agent i , we consider a weighted Bellman backup as follows:

$$\begin{aligned} \mathcal{L}_{WQ}(\tau_t, \theta_i) &= w(s_{t+1}, a_{t+1}) (Q_{\theta_i}(s_t, a_t) - r_t - \gamma (Q_{\bar{\theta}_i}(s_{t+1}, a_{t+1}) - \alpha \log \pi_{\phi}(a_{t+1}|s_{t+1})))^2, \end{aligned} \quad (4)$$

where $\tau_t = (s_t, a_t, r_t, s_{t+1})$ is a transition, $a_{t+1} \sim \pi_{\phi}(a|s_t)$, and $w(s, a)$ is a confidence weight based on ensemble of target Q-functions:

$$w(s, a) = \sigma(-\bar{Q}_{\text{std}}(s, a) * T) + 0.5, \quad (5)$$

where $T > 0$ is a temperature, σ is the sigmoid function, and $\bar{Q}_{\text{std}}(s, a)$ is the empirical standard deviation of all target Q-functions $\{Q_{\bar{\theta}_i}\}_{i=1}^N$. Note that the confidence weight is bounded in $[0.5, 1.0]$ because standard deviation is always positive.² The proposed objective \mathcal{L}_{WQ} down-weights the sample transitions with high variance across target Q-functions, resulting in a loss function for the Q updates that has a better signal-to-noise ratio.

UCB exploration. The ensemble can also be leveraged for efficient exploration [10, 33] because it can express higher uncertainty on unseen samples. Motivated by this, by following the idea of Chen et al. [10], we consider an optimism-based exploration that chooses the action that maximizes

$$a_t = \max_a \{Q_{\text{mean}}(s_t, a) + \lambda Q_{\text{std}}(s_t, a)\}, \quad (6)$$

²We find that it is empirically stable to set minimum value of weight $w(s, a)$ as 0.5.

where $Q_{\text{mean}}(s, a)$ and $Q_{\text{std}}(s, a)$ are the empirical mean and standard deviation of all Q-functions $\{Q_{\theta_i}\}_{i=1}^N$, and the $\lambda > 0$ is a hyperparameter. This inference method can encourage exploration by adding an exploration bonus (i.e., standard deviation Q_{std}) for visiting unseen state-action pairs similar to the UCB algorithm [4]. We remark that this inference method was originally proposed in Chen et al. [10] for efficient exploration in discrete action spaces. However, in continuous action spaces, finding the action that maximizes the UCB is not straightforward. To handle this issue, we propose a simple approximation scheme, which first generates N candidate action set from ensemble policies $\{\pi_{\phi_i}\}_{i=1}^N$, and then chooses the action that maximizes the UCB (Line 4 in Algorithm 1). For evaluation, we approximate the maximum a posterior action by averaging the mean of Gaussian distributions modeled by each ensemble policy. The full procedure is summarized in Algorithm 1.

4 Experimental results

We designed our experiments to answer the following questions:

- Can SUNRISE improve off-policy RL algorithms, such as SAC [15] and Rainbow DQN [20], for both continuous (see Table 1 and Table 2) and discrete (see Table 3) control tasks?
- Does SUNRISE mitigate error propagation (see Figure 2(a))?
- How does ensemble size affect the performance of SUNRISE (see Figure 2(b) and Figure 2(c))?
- What is the contribution of each technique in SUNRISE (see Table 4)?

4.1 Setups

Continuous control tasks. We evaluate SUNRISE on several continuous control tasks using simulated robots from OpenAI Gym [9] and DeepMind Control Suite [43]. For OpenAI Gym experiments with proprioceptive inputs (e.g., positions and velocities), we compare to PETS [12], a state-of-the-art model-based RL method based on ensembles of dynamics models; POPLIN-P [49], a state-of-the-art model-based RL method which uses a policy network to generate actions for planning; POPLIN-A [49], variant of POPLIN-P which adds noise in the action space; METRPO [28], a hybrid RL method which augments TRPO [36] using ensembles of dynamics models; and two state-of-the-art model-free RL methods, TD3 [14] and SAC [15]. For our method, we consider a combination of SAC and SUNRISE, as described in Algorithm 1. Following the setup in POPLIN [49], we report the mean and standard deviation across four runs after 200K timesteps on four complex environments: Cheetah, Walker, Hopper, and Ant. More experimental details and learning curves are in Appendix D.

For DeepMind Control Suite with image inputs, we compare to PlaNet [16], a model-based RL method which learns a latent dynamics model and uses it for planning; Dreamer [17], a hybrid RL method which utilizes the latent dynamics model to generate synthetic roll-outs; SLAC [31], a hybrid RL method which combines the latent dynamics model with SAC; and three state-of-the-art model-free RL methods which apply contrastive learning (CURL [41]) or data augmentation (RAD [30] and DrQ [25]) to SAC. For our method, we consider a combination of RAD (i.e., SAC with random crop) and SUNRISE. Following the setup in RAD [30], we report the mean and standard deviation across five runs after 100k (i.e., low sample regime) and 500k (i.e., asymptotically optimal regime) environment steps on six environments: Finger-spin, Cartpole-swing, Reacher-easy, Cheetah-run, Walker-walk, and Cup-catch. More experimental details and learning curves are in Appendix E.

Discrete control benchmarks. For discrete control tasks, we demonstrate the effectiveness of SUNRISE on several Atari games [6]. We compare to SimPLe [23], a hybrid RL method which updates the policy only using samples generated by learned dynamics model; Rainbow DQN [20] with modified hyperparameters for sample-efficiency [47]; Random agent [23]; CURL [41]; a model-free RL method which applies the contrastive learning to Rainbow DQN; and Human performances reported in Kaiser et al. [23] and van Hasselt et al. [47]. Following the setups in SimPLe [23], we report the mean across three runs after 100K interactions (i.e., 400K frames with action repeat of 4). For our method, we consider a combination of sample-efficient versions of Rainbow DQN [47] and SUNRISE (see Algorithm 3 in Appendix B). More experimental details and learning curves are in Appendix F.

For our method, we do not alter any hyperparameters of the original off-policy RL algorithms and train five ensemble agents. There are only three additional hyperparameters β , T , and λ for bootstrap, weighted Bellman backup, and UCB exploration, where we provide details in Appendix D, E, and F.

	Cheetah	Walker	Hopper	Ant
PETS [12]	2288.4 \pm 1019.0	282.5 \pm 501.6	114.9 \pm 621.0	1165.5 \pm 226.9
POPLIN-A [49]	1562.8 \pm 1136.7	-105.0 \pm 249.8	202.5 \pm 962.5	1148.4 \pm 438.3
POPLIN-P [49]	4235.0 \pm 1133.0	597.0 \pm 478.8	2055.2 \pm 613.8	2330.1 \pm 320.9
METRPO [28]	2283.7 \pm 900.4	-1609.3 \pm 657.5	1272.5 \pm 500.9	282.2 \pm 18.0
TD3 [14]	3015.7 \pm 969.8	-516.4 \pm 812.2	1816.6 \pm 994.8	870.1 \pm 283.8
SAC [15]	4035.7 \pm 268.0	-382.5 \pm 849.5	2020.6 \pm 692.9	836.5 \pm 68.4
SUNRISE	5370.6 \pm 483.1	1926.5 \pm 694.8	2601.9 \pm 306.5	1627.0 \pm 292.7

Table 1: Performance on OpenAI Gym at 200K timesteps. The results show the mean and standard deviation averaged over four runs, and the best results are indicated in bold. For baseline methods, we report the best number in POPLIN [49].

500K step	PlaNet [16]	Dreamer [17]	SLAC [31]	CURL [41]	DrQ [25]	RAD [30]	SUNRISE
Finger-spin	561 \pm 284	796 \pm 183	673 \pm 92	926 \pm 45	938 \pm 103	975 \pm 16	983 \pm 1
Cartpole-swing	475 \pm 71	762 \pm 27	-	845 \pm 45	868 \pm 10	873 \pm 3	876 \pm 4
Reacher-easy	210 \pm 44	793 \pm 164	-	929 \pm 44	942 \pm 71	916 \pm 49	982 \pm 3
Cheetah-run	305 \pm 131	570 \pm 253	640 \pm 19	518 \pm 28	660 \pm 96	624 \pm 10	678 \pm 46
Walker-walk	351 \pm 58	897 \pm 49	842 \pm 51	902 \pm 43	921 \pm 45	938 \pm 9	953 \pm 13
Cup-catch	460 \pm 380	879 \pm 87	852 \pm 71	959 \pm 27	963 \pm 9	966 \pm 9	969 \pm 5
100K step							
Finger-spin	136 \pm 216	341 \pm 70	693 \pm 141	767 \pm 56	901 \pm 104	811 \pm 146	905 \pm 57
Cartpole-swing	297 \pm 39	326 \pm 27	-	582 \pm 146	759 \pm 92	373 \pm 90	591 \pm 55
Reacher-easy	20 \pm 50	314 \pm 155	-	538 \pm 233	601 \pm 213	567 \pm 54	722 \pm 50
Cheetah-run	138 \pm 88	235 \pm 137	319 \pm 56	299 \pm 48	344 \pm 67	381 \pm 79	413 \pm 35
Walker-walk	224 \pm 48	277 \pm 12	361 \pm 73	403 \pm 24	612 \pm 164	641 \pm 89	667 \pm 147
Cup-catch	0 \pm 0	246 \pm 174	512 \pm 110	769 \pm 43	913 \pm 53	666 \pm 181	633 \pm 241

Table 2: Performance on DeepMind Control Suite at 100K and 500K environment steps. The results show the mean and standard deviation averaged five runs, and the best results are indicated in bold. For baseline methods, we report the best numbers reported in prior works [25, 30].

4.2 Comparative evaluation

OpenAI Gym. Table 1 shows the average returns of evaluation roll-outs for all methods. SUNRISE consistently improves the performance of SAC across all environments and outperforms the state-of-the-art POPLIN-P on all environments except Ant. In particular, the average returns are improved from 597.0 to 1926.5 compared to POPLIN-P on the Walker environment, which most model-based RL methods cannot solve efficiently. We remark that SUNRISE is more compute-efficient than modern model-based RL methods, such as POPLIN and PETS, because they also utilize ensembles (of dynamics models) and perform planning to select actions. Namely, SUNRISE is simple to implement, computationally efficient, and readily parallelizable.

DeepMind Control Suite. As shown in Table 2, SUNRISE also consistently improves the performance of RAD (i.e., SAC with random crop) on all environments from DeepMind Control Suite. This implies that the proposed method can be useful for high-dimensional and complex input observations. Moreover, our method achieves state-of-the-art performances in almost all environments against existing pixel-based RL methods. We remark that SUNRISE can also be combined with DrQ, and expect that it can achieve better performances on Cartpole-swing and Cup-catch at 100K environment steps.

Atari games. We also evaluate SUNRISE on discrete control tasks using Rainbow DQN on Atari games. Table 3 shows that SUNRISE improves the performance of Rainbow in almost all environments, and achieves state-of-the-art performance on 12 out of 26 environments. Here, we remark that SUNRISE is also compatible with CURL, which could enable even better performance. These results demonstrate that SUNRISE is a general approach, and can be applied to various off-policy RL algorithms.

Game	Human	Random	SimPLe [23]	CURL [41]	Rainbow [47]	SUNRISE
Alien	7127.7	227.8	616.9	558.2	789.0	872.0
Amidar	1719.5	5.8	88.0	142.1	118.5	122.6
Assault	742.0	222.4	527.2	600.6	413.0	594.8
Asterix	8503.3	210.0	1128.3	734.5	533.3	755.0
BankHeist	753.1	14.2	34.2	131.6	97.7	266.7
BattleZone	37187.5	2360.0	5184.4	14870.0	7833.3	15700.0
Boxing	12.1	0.1	9.1	1.2	0.6	6.7
Breakout	30.5	1.7	16.4	4.9	2.3	1.8
ChopperCommand	7387.8	811.0	1246.9	1058.5	590.0	1040.0
CrazyClimber	35829.4	10780.5	62583.6	12146.5	25426.7	22230.0
DemonAttack	1971.0	152.1	208.1	817.6	688.2	919.8
Freeway	29.6	0.0	20.3	26.7	28.7	30.2
Frostbite	4334.7	65.2	254.7	1181.3	1478.3	2026.7
Gopher	2412.5	257.6	771.0	669.3	348.7	654.7
Hero	30826.4	1027.0	2656.6	6279.3	3675.7	8072.5
Jamesbond	302.8	29.0	125.3	471.0	300.0	390.0
Kangaroo	3035.0	52.0	323.1	872.5	1060.0	2000.0
Krull	2665.5	1598.0	4539.9	4229.6	2592.1	3087.2
KungFuMaster	22736.3	258.5	17257.2	14307.8	8600.0	10306.7
MsPacman	6951.6	307.3	1480.0	1465.5	1118.7	1482.3
Pong	14.6	-20.7	12.8	-16.5	-19.0	-19.3
PrivateEye	69571.3	24.9	58.3	218.4	97.8	100.0
Qbert	13455.0	163.9	1288.8	1042.4	646.7	1830.8
RoadRunner	7845.0	11.5	5640.6	5661.0	9923.3	11913.3
Seaquest	42054.7	68.4	683.3	384.5	396.0	570.7
UpNDown	11693.2	533.4	3350.3	2955.2	3816.0	5074.0

Table 3: Performance on Atari games at 100K interactions. The results show the scores averaged three runs, and the best results are indicated in bold. For baseline methods, we report the best numbers reported in prior works [23, 47].

OpenAI Gym with stochastic rewards. To verify the effectiveness of SUNRISE in mitigating error propagation, following Kumar et al. [26], we evaluate on a modified version of OpenAI Gym environments with stochastic rewards by adding Gaussian noise to the reward function: $r'(s, a) = r(s, a) + z$, where $z \sim \mathcal{N}(0, 1)$. This increases the noise in value estimates. Following Kumar et al. [26], we only inject this noisy reward during training and report the deterministic ground-truth reward during evaluation. For our method, we also consider a variant of SUNRISE, which selects action without UCB exploration to isolate the effect of the proposed weighted Bellman backup. Specifically, we randomly select an index of policy uniformly at random and generate actions from the selected policy for the duration of that episode similar to Bootstrapped DQN [33] (see Algorithm 2 in Appendix A). Our method is compared with DisCor [27], which improves SAC by reweighting the Bellman backup based on estimated cumulative Bellman errors (see Appendix G for more details).

Figure 2(a) shows the learning curves of all methods on the Cheetah environment with stochastic rewards. SUNRISE outperforms baselines such as SAC and DisCor, even when only using the proposed weighted Bellman backup (green curve). This implies that errors in the target Q-function can be characterized by the proposed confident weight in (5) effectively. By additionally utilizing UCB exploration, both sample-efficiency and asymptotic performance of SUNRISE are further improved (blue curve). More evaluation results with DisCor on other environments are also available in Appendix G, where the overall trend is similar.

4.3 Ablation study

Effects of ensemble size. We analyze the effects of ensemble size N on the Cheetah and Ant environments from OpenAI Gym. Figure 2(b) and Figure 2(c) show that the performance can be improved by increasing the ensemble size, but the improvement is saturated around $N = 5$. Thus, we use five ensemble agents for all experiments. More experimental results on the Hopper and Walker environments are also available in Appendix D, where the overall trend is similar.

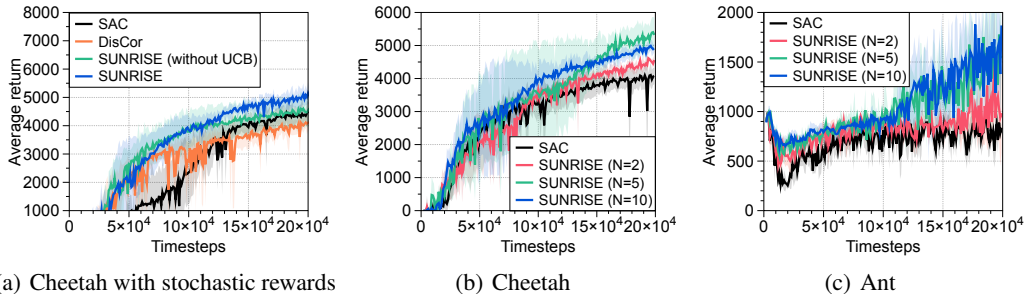


Figure 2: (a) Comparison with DisCor on modified Cheetah environment, where we add Gaussian noise to reward function to increase an error in value estimations. Learning curves of SUNRISE with varying values of ensemble size N on (b) Cheetah and (c) Ant environments.

Atari games	BOOT	WB	UCB	Seaquest	ChopperCommand	Gopher
Rainbow	-	-	-	396.0 ± 37.7	590.0 ± 127.3	348.7 ± 43.8
SUNRISE	✓	-	-	547.3 ± 110.0	590.0 ± 85.2	222.7 ± 34.7
	✓	✓	-	550.7 ± 67.0	860.0 ± 235.5	377.3 ± 195.6
	✓	-	✓	477.3 ± 48.5	623.3 ± 216.4	286.0 ± 39.2
	✓	✓	✓	570.7 ± 43.6	1040.0 ± 77.9	654.7 ± 218.0
OpenAI Gym	BOOT	WB	UCB	Cheetah	Hopper	Ant
SAC	-	-	-	4035.7 ± 268.0	2020.6 ± 692.9	836.5 ± 68.4
SUNRISE	✓	-	-	4213.5 ± 249.1	2378.3 ± 538.0	1033.4 ± 106.0
	✓	✓	-	5197.4 ± 448.1	2586.5 ± 317.0	1164.6 ± 488.4
	✓	-	✓	4789.3 ± 192.3	2393.2 ± 316.9	1684.8 ± 1060.9
	✓	✓	✓	5370.6 ± 483.1	2601.9 ± 306.5	1627.0 ± 292.7

Table 4: Contribution of each technique in SUNRISE, i.e., bootstrap with random initialization (BOOT), weighted Bellman backup (WB), and UCB exploration, on several environments from OpenAI Gym and Atari games at 200K timesteps and 100K interactions. The results show the mean and standard deviation averaged over four and three runs for OpenAI Gym and Atari games.

Contribution of each technique. In order to verify the individual effects of each technique in SUNRISE, we incrementally apply our techniques. For SUNRISE without UCB exploration, we use random inference proposed in Bootstrapped DQN [33], which randomly selects an index of policy uniformly at random and generates the action from the selected actor for the duration of that episode (see Algorithm 2 in Appendix A). Table 4 shows the performance of SUNRISE on several environments from OpenAI Gym and Atari games. First, we remark that the performance gain from SUNRISE only with bootstrap, which corresponds to a naive extension of Bootstrap DQN [33], is marginal compared to other techniques, such as weighted Bellman backup and UCB exploration. However, by utilizing all proposed techniques, we obtain the best performance in almost all environments. This shows that all proposed techniques can be integrated and that they are indeed largely complementary.

5 Conclusion

In this paper, we present SUNRISE, a simple unified ensemble method, which is compatible with various off-policy RL algorithms. In particular, SUNRISE integrates bootstrap with random initialization, weighted Bellman backup, and UCB exploration to handle various issues in off-policy RL algorithms. Our experiments show that SUNRISE consistently improves the performances of existing off-policy RL algorithms, such as Soft Actor-Critic and Rainbow DQN, and outperforms state-of-the-art RL algorithms for both continuous and discrete control tasks on both low-dimensional and high-dimensional environments. We believe that SUNRISE could be useful to other relevant topics such as sim-to-real transfer [44], imitation learning [45], offline RL [1], and planning [40, 42].

Acknowledgements

This research is supported in part by ONR PECASE N000141612723, Tencent, and Berkeley Deep Drive. We would like to thank Hao Liu for improving the presentation and giving helpful feedback. We would also like to thank Aviral Kumar and Kai Arulkumaran for providing tips on implementation of DisCor and Rainbow.

Broader Impact

Despite impressive progress in Deep RL over the last few years, a number of issues prevent RL algorithms from being deployed to real-world problems like autonomous navigation [8] and industrial robotic manipulation [24]. One issue, among several others, is training stability. RL algorithms are often sensitive to hyperparameters, noisy, and converge at suboptimal policies. Our work addresses the stability issue by providing a unified framework for utilizing ensembles during training. The resulting algorithm significantly improves the stability of prior methods. Though we demonstrate results on common RL benchmarks, SUNRISE could be one component, of many, that helps stabilize training RL policies in the real-world tasks like robotically assisted elderly care, automation of household tasks, and robotic assembly in manufacturing.

One downside to the SUNRISE method is that it requires additional compute proportional to the ensemble size. A concern is that developing methods that require increased computing resources to improve performance and deploying them at scale could lead to increased carbon emissions due to the energy required to power large compute clusters [37]. For this reason, it is also important to develop complementary methods for training large networks energy-efficiently [22].

References

- [1] Agarwal, Rishabh, Schuurmans, Dale, and Norouzi, Mohammad. An optimistic perspective on offline reinforcement learning. In *ICML*, 2020.
- [2] Anschel, Oron, Baram, Nir, and Shimkin, Nahum. Averaged-dqn: Variance reduction and stabilization for deep reinforcement learning. In *ICML*, 2017.
- [3] Audibert, Jean-Yves, Munos, Rémi, and Szepesvári, Csaba. Exploration–exploitation tradeoff using variance estimates in multi-armed bandits. *Theoretical Computer Science*, 410(19): 1876–1902, 2009.
- [4] Auer, Peter, Cesa-Bianchi, Nicolo, and Fischer, Paul. Finite-time analysis of the multiarmed bandit problem. *Machine learning*, 47(2-3):235–256, 2002.
- [5] Bellemare, Marc, Srinivasan, Sriram, Ostrovski, Georg, Schaul, Tom, Saxton, David, and Munos, Remi. Unifying count-based exploration and intrinsic motivation. In *NeurIPS*, 2016.
- [6] Bellemare, Marc G, Naddaf, Yavar, Veness, Joel, and Bowling, Michael. The arcade learning environment: An evaluation platform for general agents. *Journal of Artificial Intelligence Research*, 47:253–279, 2013.
- [7] Bellemare, Marc G, Dabney, Will, and Munos, Rémi. A distributional perspective on reinforcement learning. In *ICML*, 2017.
- [8] Bojarski, Mariusz, Del Testa, Davide, Dworakowski, Daniel, Firner, Bernhard, Flepp, Beat, Goyal, Prasoon, Jackel, Lawrence D, Monfort, Mathew, Muller, Urs, Zhang, Jiakai, et al. End to end learning for self-driving cars. *arXiv preprint arXiv:1604.07316*, 2016.
- [9] Brockman, Greg, Cheung, Vicki, Pettersson, Ludwig, Schneider, Jonas, Schulman, John, Tang, Jie, and Zaremba, Wojciech. Openai gym. *arXiv preprint arXiv:1606.01540*, 2016.
- [10] Chen, Richard Y, Sidor, Szymon, Abbeel, Pieter, and Schulman, John. Ucb exploration via q-ensembles. *arXiv preprint arXiv:1706.01502*, 2017.
- [11] Choi, Jongwook, Guo, Yijie, Moczulski, Marcin, Oh, Junhyuk, Wu, Neal, Norouzi, Mohammad, and Lee, Honglak. Contingency-aware exploration in reinforcement learning. In *ICLR*, 2019.

- [12] Chua, Kurtland, Calandra, Roberto, McAllister, Rowan, and Levine, Sergey. Deep reinforcement learning in a handful of trials using probabilistic dynamics models. In *NeurIPS*, 2018.
- [13] Efron, Bradley. *The jackknife, the bootstrap, and other resampling plans*, volume 38. Siam, 1982.
- [14] Fujimoto, Scott, Van Hoof, Herke, and Meger, David. Addressing function approximation error in actor-critic methods. In *ICML*, 2018.
- [15] Haarnoja, Tuomas, Zhou, Aurick, Abbeel, Pieter, and Levine, Sergey. Soft actor-critic: Off-policy maximum entropy deep reinforcement learning with a stochastic actor. In *ICML*, 2018.
- [16] Hafner, Danijar, Lillicrap, Timothy, Fischer, Ian, Villegas, Ruben, Ha, David, Lee, Honglak, and Davidson, James. Learning latent dynamics for planning from pixels. In *ICML*, 2019.
- [17] Hafner, Danijar, Lillicrap, Timothy, Ba, Jimmy, and Norouzi, Mohammad. Dream to control: Learning behaviors by latent imagination. In *ICLR*, 2020.
- [18] Hasselt, Hado V. Double q-learning. In *NeurIPS*, 2010.
- [19] Henderson, Peter, Islam, Riashat, Bachman, Philip, Pineau, Joelle, Precup, Doina, and Meger, David. Deep reinforcement learning that matters. In *AAAI*, 2018.
- [20] Hessel, Matteo, Modayil, Joseph, Van Hasselt, Hado, Schaul, Tom, Ostrovski, Georg, Dabney, Will, Horgan, Dan, Piot, Bilal, Azar, Mohammad, and Silver, David. Rainbow: Combining improvements in deep reinforcement learning. In *AAAI*, 2018.
- [21] Houthoofd, Rein, Chen, Xi, Duan, Yan, Schulman, John, De Turck, Filip, and Abbeel, Pieter. Vime: Variational information maximizing exploration. In *NeurIPS*, 2016.
- [22] Howard, Andrew G, Zhu, Menglong, Chen, Bo, Kalenichenko, Dmitry, Wang, Weijun, Weyand, Tobias, Andreetto, Marco, and Adam, Hartwig. Mobilenets: Efficient convolutional neural networks for mobile vision applications. *arXiv preprint arXiv:1704.04861*, 2017.
- [23] Kaiser, Lukasz, Babaeizadeh, Mohammad, Milos, Piotr, Osinski, Blazej, Campbell, Roy H, Czechowski, Konrad, Erhan, Dumitru, Finn, Chelsea, Kozakowski, Piotr, Levine, Sergey, et al. Model-based reinforcement learning for atari. In *ICLR*, 2020.
- [24] Kalashnikov, Dmitry, Irpan, Alex, Pastor, Peter, Ibarz, Julian, Herzog, Alexander, Jang, Eric, Quillen, Deirdre, Holly, Ethan, Kalakrishnan, Mrinal, Vanhoucke, Vincent, et al. Qt-opt: Scalable deep reinforcement learning for vision-based robotic manipulation. In *CoRL*, 2018.
- [25] Kostrikov, Ilya, Yarats, Denis, and Fergus, Rob. Image augmentation is all you need: Regularizing deep reinforcement learning from pixels. *arXiv preprint arXiv:2004.13649*, 2020.
- [26] Kumar, Aviral, Fu, Justin, Soh, Matthew, Tucker, George, and Levine, Sergey. Stabilizing off-policy q-learning via bootstrapping error reduction. In *NeurIPS*, 2019.
- [27] Kumar, Aviral, Gupta, Abhishek, and Levine, Sergey. Discor: Corrective feedback in reinforcement learning via distribution correction. *arXiv preprint arXiv:2003.07305*, 2020.
- [28] Kurutach, Thanard, Clavera, Ignasi, Duan, Yan, Tamar, Aviv, and Abbeel, Pieter. Model-ensemble trust-region policy optimization. In *ICLR*, 2018.
- [29] Lan, Qingfeng, Pan, Yangchen, Fyshe, Alona, and White, Martha. Maxmin q-learning: Controlling the estimation bias of q-learning. In *ICLR*, 2020.
- [30] Laskin, Michael, Lee, Kimin, Stooke, Adam, Pinto, Lerrel, Abbeel, Pieter, and Srinivas, Aravind. Reinforcement learning with augmented data. *arXiv preprint arXiv:2004.14990*, 2020.
- [31] Lee, Alex X, Nagabandi, Anusha, Abbeel, Pieter, and Levine, Sergey. Stochastic latent actor-critic: Deep reinforcement learning with a latent variable model. *arXiv preprint arXiv:1907.00953*, 2019.

- [32] Mnih, Volodymyr, Kavukcuoglu, Koray, Silver, David, Rusu, Andrei A, Veness, Joel, Bellemare, Marc G, Graves, Alex, Riedmiller, Martin, Fidjeland, Andreas K, Ostrovski, Georg, et al. Human-level control through deep reinforcement learning. *Nature*, 518(7540):529, 2015.
- [33] Osband, Ian, Blundell, Charles, Pritzel, Alexander, and Van Roy, Benjamin. Deep exploration via bootstrapped dqn. In *NeurIPS*, 2016.
- [34] Pathak, Deepak, Agrawal, Pulkit, Efros, Alexei A, and Darrell, Trevor. Curiosity-driven exploration by self-supervised prediction. In *ICML*, 2017.
- [35] Schaul, Tom, Quan, John, Antonoglou, Ioannis, and Silver, David. Prioritized experience replay. In *ICLR*, 2016.
- [36] Schulman, John, Levine, Sergey, Abbeel, Pieter, Jordan, Michael, and Moritz, Philipp. Trust region policy optimization. In *ICML*, 2015.
- [37] Schwartz, Michael O. Groundwater contamination associated with a potential nuclear waste repository at yucca mountain, usa. *Bulletin of Engineering Geology and the Environment*, 79(2):1125–1136, 2020.
- [38] Silver, David, Schrittwieser, Julian, Simonyan, Karen, Antonoglou, Ioannis, Huang, Aja, Guez, Arthur, Hubert, Thomas, Baker, Lucas, Lai, Matthew, Bolton, Adrian, et al. Mastering the game of go without human knowledge. *Nature*, 550(7676):354, 2017.
- [39] Silver, David, Hubert, Thomas, Schrittwieser, Julian, Antonoglou, Ioannis, Lai, Matthew, Guez, Arthur, Lanctot, Marc, Sifre, Laurent, Kumaran, Dharshan, Graepel, Thore, et al. A general reinforcement learning algorithm that masters chess, shogi, and go through self-play. *Science*, 362(6419):1140–1144, 2018.
- [40] Srinivas, Aravind, Jabri, Allan, Abbeel, Pieter, Levine, Sergey, and Finn, Chelsea. Universal planning networks. *arXiv preprint arXiv:1804.00645*, 2018.
- [41] Srinivas, Aravind, Laskin, Michael, and Abbeel, Pieter. Curl: Contrastive unsupervised representations for reinforcement learning. In *ICML*, 2020.
- [42] Tamar, Aviv, Wu, Yi, Thomas, Garrett, Levine, Sergey, and Abbeel, Pieter. Value iteration networks. In *NeurIPS*, 2016.
- [43] Tassa, Yuval, Doron, Yotam, Muldal, Alistair, Erez, Tom, Li, Yazhe, Casas, Diego de Las, Budden, David, Abdolmaleki, Abbas, Merel, Josh, Lefrancq, Andrew, et al. Deepmind control suite. *arXiv preprint arXiv:1801.00690*, 2018.
- [44] Tobin, Josh, Fong, Rachel, Ray, Alex, Schneider, Jonas, Zaremba, Wojciech, and Abbeel, Pieter. Domain randomization for transferring deep neural networks from simulation to the real world. In *IROS*, 2017.
- [45] Torabi, Faraz, Warnell, Garrett, and Stone, Peter. Behavioral cloning from observation. In *IJCAI*, 2018.
- [46] Van Hasselt, Hado, Guez, Arthur, and Silver, David. Deep reinforcement learning with double q-learning. In *AAAI*, 2016.
- [47] van Hasselt, Hado P, Hessel, Matteo, and Aslanides, John. When to use parametric models in reinforcement learning? In *NeurIPS*, 2019.
- [48] Vinyals, Oriol, Babuschkin, Igor, Czarnecki, Wojciech M, Mathieu, Michael, Dudzik, Andrew, Chung, Junyoung, Choi, David H, Powell, Richard, Ewalds, Timo, Georgiev, Petko, et al. Grandmaster level in starcraft ii using multi-agent reinforcement learning. *Nature*, 575(7782): 350–354, 2019.
- [49] Wang, Tingwu and Ba, Jimmy. Exploring model-based planning with policy networks. In *ICLR*, 2020.

- [50] Wang, Tingwu, Bao, Xuchan, Clavera, Ignasi, Hoang, Jerrick, Wen, Yeming, Langlois, Eric, Zhang, Shunshi, Zhang, Guodong, Abbeel, Pieter, and Ba, Jimmy. Benchmarking model-based reinforcement learning. *arXiv preprint arXiv:1907.02057*, 2019.
- [51] Wiering, Marco A and Van Hasselt, Hado. Ensemble algorithms in reinforcement learning. *IEEE Transactions on Systems, Man, and Cybernetics*, 38(4):930–936, 2008.
- [52] Yarats, Denis, Zhang, Amy, Kostrikov, Ilya, Amos, Brandon, Pineau, Joelle, and Fergus, Rob. Improving sample efficiency in model-free reinforcement learning from images. *arXiv preprint arXiv:1910.01741*, 2019.
- [53] Ziebart, Brian D. Modeling purposeful adaptive behavior with the principle of maximum causal entropy. 2010.

Appendix:

SUNRISE: A Simple Unified Framework for Ensemble Learning in Deep Reinforcement Learning

A SUNRISE: Soft actor-critic

Background. SAC [15] is a state-of-the-art off-policy algorithm for continuous control problems. SAC learns a policy, $\pi_\phi(a|s)$, and a critic, $Q_\theta(s, a)$, and aims to maximize a weighted objective of the reward and the policy entropy, $\mathbb{E}_{s_t, a_t \sim \pi} [\sum_t \gamma^{t-1} r_t + \alpha \mathcal{H}(\pi_\phi(\cdot|s_t))]$. To update the parameters, SAC alternates between a soft policy evaluation and a soft policy improvement. At the soft policy evaluation step, a soft Q-function, which is modeled as a neural network with parameters θ , is updated by minimizing the following soft Bellman residual:

$$\begin{aligned} \mathcal{L}_{\text{critic}}^{\text{SAC}}(\theta) &= \mathbb{E}_{\tau_t \sim \mathcal{B}} [\mathcal{L}_Q(\tau_t, \theta)], \\ \mathcal{L}_Q(\tau_t, \theta) &= (Q_\theta(s_t, a_t) - r_t - \gamma \mathbb{E}_{a_{t+1} \sim \pi_\phi} [Q_{\bar{\theta}}(s_{t+1}, a_{t+1}) - \alpha \log \pi_\phi(a_{t+1}|s_{t+1})])^2, \end{aligned}$$

where $\tau_t = (s_t, a_t, r_t, s_{t+1})$ is a transition, \mathcal{B} is a replay buffer, $\bar{\theta}$ are the delayed parameters, and α is a temperature parameter. At the soft policy improvement step, the policy π with its parameter ϕ is updated by minimizing the following objective:

$$\mathcal{L}_{\text{actor}}^{\text{SAC}}(\phi) = \mathbb{E}_{s_t \sim \mathcal{B}} [\mathcal{L}_\pi(s_t, \phi)], \text{ where } \mathcal{L}_\pi(s_t, \phi) = \mathbb{E}_{a_t \sim \pi_\phi} [\alpha \log \pi_\phi(a_t|s_t) - Q_\theta(s_t, a_t)].$$

We remark that this corresponds to minimizing the Kullback-Leibler divergence between the policy and a Boltzmann distribution induced by the current soft Q-function.

SUNRISE without UCB exploration. For SUNRISE without UCB exploration, we use random inference proposed in Bootstrapped DQN [33], which randomly selects an index of policy uniformly at random and generates the action from the selected actor for the duration of that episode (see Line 3 in Algorithm 2).

Algorithm 2 SUNRISE: SAC version (random inference)

```
1: for each iteration do
2:   // RANDOM INFERENCE
3:   Select an index of policy using  $\hat{i} \sim \text{Uniform}\{1, \dots, N\}$ 
4:   for each timestep  $t$  do
5:     Get the action from selected policy:  $a_t \sim \pi_{\phi_{\hat{i}}}(a|s_t)$ 
6:     Collect state  $s_{t+1}$  and reward  $r_t$  from the environment by taking action  $a_t$ 
7:     Sample bootstrap masks  $M_t = \{m_{t,i} \sim \text{Bernoulli}(\beta) \mid i \in \{1, \dots, N\}\}$ 
8:     Store transitions  $\tau_t = (s_t, a_t, s_{t+1}, r_t)$  and masks in replay buffer  $\mathcal{B} \leftarrow \mathcal{B} \cup \{(\tau_t, M_t)\}$ 
9:   end for
10:  // UPDATE AGENTS VIA BOOTSTRAP AND WEIGHTED BELLMAN BACKUP
11:  for each gradient step do
12:    Sample random minibatch  $\{(\tau_j, M_j)\}_{j=1}^B \sim \mathcal{B}$ 
13:    for each agent  $i$  do
14:      Update the Q-function by minimizing  $\frac{1}{B} \sum_{j=1}^B m_{j,i} \mathcal{L}_{WQ}(\tau_j, \theta_i)$ 
15:      Update the policy by minimizing  $\frac{1}{B} \sum_{j=1}^B m_{j,i} \mathcal{L}_\pi(s_j, \phi_i)$ 
16:    end for
17:  end for
18: end for
```

B Extension to Rainbow DQN

B.1 Preliminaries: Rainbow DQN

Background. DQN algorithm [32] learns a Q-function, which is modeled as a neural network with parameters θ , by minimizing the following Bellman residual:

$$\mathcal{L}^{\text{DQN}}(\theta) = \mathbb{E}_{\tau_t \sim \mathcal{B}} \left[\left(Q_\theta(s_t, a_t) - r_t - \gamma \max_a Q_{\bar{\theta}}(s_{t+1}, a) \right)^2 \right], \quad (7)$$

where $\tau_t = (s_t, a_t, r_t, s_{t+1})$ is a transition, \mathcal{B} is a replay buffer, and $\bar{\theta}$ are the delayed parameters. Even though Rainbow DQN integrates several techniques, such as double Q-learning [46] and distributional DQN [7], applying SUNRISE to Rainbow DQN can be described based on the standard DQN algorithm. For exposition, we refer the reader to Hessel et al. [20] for more detailed explanations of Rainbow DQN.

B.2 SUNRISE: Rainbow DQN

Bootstrap with random initialization. Formally, we consider an ensemble of N Q-functions, i.e., $\{Q_{\theta_i}\}_{i=1}^N$, where θ_i denotes the parameters of the i -th Q-function.³ To train the ensemble of Q-functions, we use the bootstrap with random initialization [13, 33], which enforces the diversity between Q-functions through two simple ideas: First, we initialize the model parameters of all Q-functions with random parameter values for inducing an initial diversity in the models. Second, we apply different samples to train each Q-function. Specifically, for each Q-function i in each timestep t , we draw the binary masks $m_{t,i}$ from the Bernoulli distribution with parameter $\beta \in (0, 1]$, and store them in the replay buffer. Then, when updating the model parameters of Q-functions, we multiply the bootstrap mask to each objective function.

Weighted Bellman backup. Since conventional Q-learning is based on the Bellman backup in (7), it can be affected by error propagation. I.e., error in the target Q-function $Q_{\bar{\theta}}(s_{t+1}, a_{t+1})$ gets propagated into the Q-function $Q_\theta(s_t, a_t)$ at the current state. Recently, Kumar et al. [27] showed that this error propagation can cause inconsistency and unstable convergence. To mitigate this issue, for each Q-function i , we consider a weighted Bellman backup as follows:

$$\mathcal{L}_{WQ}^{\text{DQN}}(\tau_t, \theta_i) = w(s_{t+1}) \left(Q_{\theta_i}(s_t, a_t) - r_t - \gamma \max_a Q_{\bar{\theta}_i}(s_{t+1}, a) \right)^2,$$

where $\tau_t = (s_t, a_t, r_t, s_{t+1})$ is a transition, and $w(s)$ is a confidence weight based on ensemble of target Q-functions:

$$w(s) = \sigma(-\bar{Q}_{\text{std}}(s) * T) + 0.5, \quad (8)$$

where $T > 0$ is a temperature, σ is the sigmoid function, and $\bar{Q}_{\text{std}}(s)$ is the empirical standard deviation of all target Q-functions $\{\max_a Q_{\bar{\theta}_i}(s, a)\}_{i=1}^N$. Note that the confidence weight is bounded in $[0.5, 1.0]$ because standard deviation is always positive.⁴ The proposed objective $\mathcal{L}_{WQ}^{\text{DQN}}$ down-weights the sample transitions with high variance across target Q-functions, resulting in a loss function for the Q updates that has a better signal-to-noise ratio. Note that we combine the proposed weighted Bellman backup with prioritized replay [35] by multiplying both weights to Bellman backups.

UCB exploration. The ensemble can also be leveraged for efficient exploration [10, 33] because it can express higher uncertainty on unseen samples. Motivated by this, by following the idea of Chen et al. [10], we consider an optimism-based exploration that chooses the action that maximizes

$$a_t = \max_a \{Q_{\text{mean}}(s_t, a) + \lambda Q_{\text{std}}(s_t, a)\}, \quad (9)$$

where $Q_{\text{mean}}(s, a)$ and $Q_{\text{std}}(s, a)$ are the empirical mean and standard deviation of all Q-functions $\{Q_{\theta_i}\}_{i=1}^N$, and the $\lambda > 0$ is a hyperparameter. This inference method can encourage exploration by adding an exploration bonus (i.e., standard deviation Q_{std}) for visiting unseen state-action pairs similar to the UCB algorithm [4]. This inference method was originally proposed in Chen et al. [10] for efficient exploration in DQN, but we further extend it to Rainbow DQN. For evaluation, we approximate the maximum a posterior action by choosing the action maximizes the mean of Q-functions, i.e., $a_t = \max_a \{Q_{\text{mean}}(s_t, a)\}$. The full procedure is summarized in Algorithm 3.

³Here, we remark that each Q-function has a unique target Q-function.

⁴We find that it is empirically stable to set minimum value of weight $w(s, a)$ as 0.5.

Algorithm 3 SUNRISE: Rainbow version

```
1: for each iteration do
2:   for each timestep  $t$  do
3:     // UCB EXPLORATION
4:     Choose the action that maximizes UCB:  $a_t = \operatorname{argmax}_{a_{t,i} \in \mathcal{A}} Q_{\text{mean}}(s_t, a_{t,i}) + \lambda Q_{\text{std}}(s_t, a_{t,i})$ 
5:     Collect state  $s_{t+1}$  and reward  $r_t$  from the environment by taking action  $a_t$ 
6:     Sample bootstrap masks  $M_t = \{m_{t,i} \sim \text{Bernoulli}(\beta) \mid i \in \{1, \dots, N\}\}$ 
7:     Store transitions  $\tau_t = (s_t, a_t, s_{t+1}, r_t)$  and masks in replay buffer  $\mathcal{B} \leftarrow \mathcal{B} \cup \{(\tau_t, M_t)\}$ 
8:   end for
9:   // UPDATE Q-FUNCTIONS VIA BOOTSTRAP AND WEIGHTED BELLMAN BACKUP
10:  for each gradient step do
11:    Sample random minibatch  $\{(\tau_j, M_j)\}_{j=1}^B \sim \mathcal{B}$ 
12:    for each agent  $i$  do
13:      Update the Q-function by minimizing  $\frac{1}{B} \sum_{j=1}^B m_{j,i} \mathcal{L}_{WQ}^{\text{DQN}}(\tau_j, \theta_i)$ 
14:    end for
15:  end for
16: end for
```

C Implementation details for toy regression tasks

We evaluate the quality of uncertainty estimates from an ensemble of neural networks on a toy regression task. To this end, we generate twenty training samples drawn as $y = x^3 + \epsilon$, where $\epsilon \sim \mathcal{N}(0, 3^2)$, and train ten ensembles of regression networks using bootstrap with random initialization. The regression network is as fully-connected neural networks with 2 hidden layers and 50 rectified linear units in each layer. For bootstrap, we draw the binary masks from the Bernoulli distribution with mean $\beta = 0.3$. As uncertainty estimates, we measure the empirical variance of the networks’ predictions. As shown in Figure 1(b), the ensemble can produce well-calibrated uncertainty estimates (i.e., variance) on unseen samples.

D Experimental setups and results: OpenAI Gym

Environments. We evaluate the performance of SUNRISE on four complex environments based on the standard bench-marking environments⁵ from OpenAI Gym [9]. Note that we do not use a modified Cheetah environments from PETS [12] (dented as Cheetah in POPLIN [49]) because it includes additional information in observations.

Training details. We consider a combination of SAC and SUNRISE using the publicly released implementation repository (<https://github.com/vitchyr/rlkit>) without any modifications on hyperparameters and architectures. For our method, the temperature for weighted Bellman backups is chosen from $T \in \{10, 20, 50\}$, the mean of the Bernoulli distribution is chosen from $\beta \in \{0.5, 1.0\}$, the penalty parameter is chosen from $\lambda \in \{1, 5, 10\}$, and we train five ensemble agents. The optimal parameters are chosen to achieve the best performance on training environments. Here, we remark that training ensemble agents using same training samples but with different initialization (i.e., $\beta = 1$) usually achieves the best performance in most cases similar to Osband et al. [33] and Chen et al. [10]. We expect that this is because splitting samples can reduce the sample-efficiency. Also, initial diversity from random initialization can be enough because each Q-function has a unique target Q-function, i.e., target value is also different according to initialization.

Learning curves. Figure 3 shows the learning curves on all environments. One can note that SUNRISE consistently improves the performance of SAC by a large margin.

Effects of ensembles. Figure 4 shows the learning curves of SUNRISE with varying values of ensemble size on all environments. The performance can be improved by increasing the ensemble size, but the improvement is saturated around $N = 5$.

⁵We used the reference implementation at <https://github.com/WilsonWangTHU/mbbl> [50].

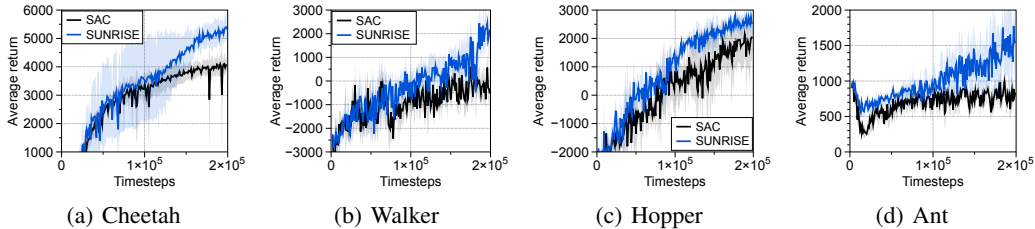


Figure 3: Learning curves on (a) Cheetah, (b) Walker, (c) Hopper, and (d) Ant environments from OpenAI Gym. The solid line and shaded regions represent the mean and standard deviation, respectively, across four runs.

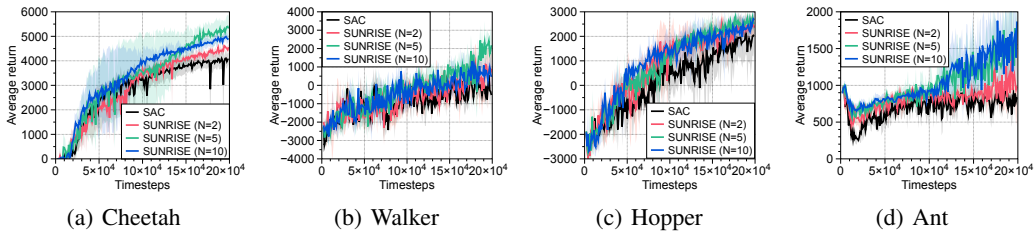


Figure 4: Learning curves of SUNRISE with varying values of ensemble size N . The solid line and shaded regions represent the mean and standard deviation, respectively, across four runs.

Hyperparameter	Value	Hyperparameter	Value
Random crop	True	Initial temperature	0.1
Observation rendering	(100, 100)	Learning rate ($f_\theta, \pi_\psi, Q_\phi$)	$2e - 4$ cheetah, run
Observation downsampling	(84, 84)		$1e - 3$ otherwise
Replay buffer size	100000	Learning rate (α)	$1e - 4$
Initial steps	1000	Batch Size	512 (cheetah), 256 (rest)
Stacked frames	3	Q function EMA τ	0.01
Action repeat	2 finger, spin; walker, walk	Critic target update freq	2
	8 cartpole, swingup	Convolutional layers	4
	4 otherwise	Number of filters	32
Hidden units (MLP)	1024	Non-linearity	ReLU
Evaluation episodes	10	Encoder EMA τ	0.05
Optimizer	Adam	Latent dimension	50
$(\beta_1, \beta_2) \rightarrow (f_\theta, \pi_\psi, Q_\phi)$	(.9, .999)	Discount γ	.99
$(\beta_1, \beta_2) \rightarrow (\alpha)$	(.5, .999)		

Table 5: Hyperparameters used for DeepMind Control Suite experiments. Most hyperparameters values are unchanged across environments with the exception for action repeat, learning rate, and batch size.

E Experimental setups and results: DeepMind Control Suite

Training details. We consider a combination of RAD and SUNRISE using the publicly released implementation repository (<https://github.com/MishaLaskin/rad>) with a full list of hyperparameters in Table 5. Similar to Laskin et al. [30], we use the same encoder architecture as in [52], and the actor and critic share the same encoder to embed image observations.⁶ For our method, the temperature for weighted Bellman backups is chosen from $T \in \{10, 100\}$, the mean of the Bernoulli distribution is chosen from $\beta \in \{0.5, 1.0\}$, the penalty parameter is chosen from $\lambda \in \{1, 5, 10\}$, and we train five ensemble agents. The optimal parameters are chosen to achieve the best performance on training environments. Here, we remark that training ensemble agents using same training samples but with different initialization (i.e., $\beta = 1$) usually achieves the best performance in most cases similar to Osband et al. [33] and Chen et al. [10]. We expect that this is because training samples

⁶However, we remark that each agent does not share the encoders unlike Bootstrapped DQN [33].

can reduce the sample-efficiency. Also, initial diversity from random initialization can be enough because each Q-function has a unique target Q-function, i.e., target value is also different according to initialization.

Learning curves. Figure 5(g), 5(h), 5(i), 5(j), 5(k), and 5(l) show the learning curves on all environments. Since RAD already achieves the near optimal performances and the room for improvement is small, we can see a small but consistent gains from SUNRISE. To verify the effectiveness of SUNRISE more clearly, we consider a combination of SAC and SUNRISE in Figure 5(a), 5(b), 5(c), 5(d), 5(e), and 5(f), where the gain from SUNRISE is more significant.

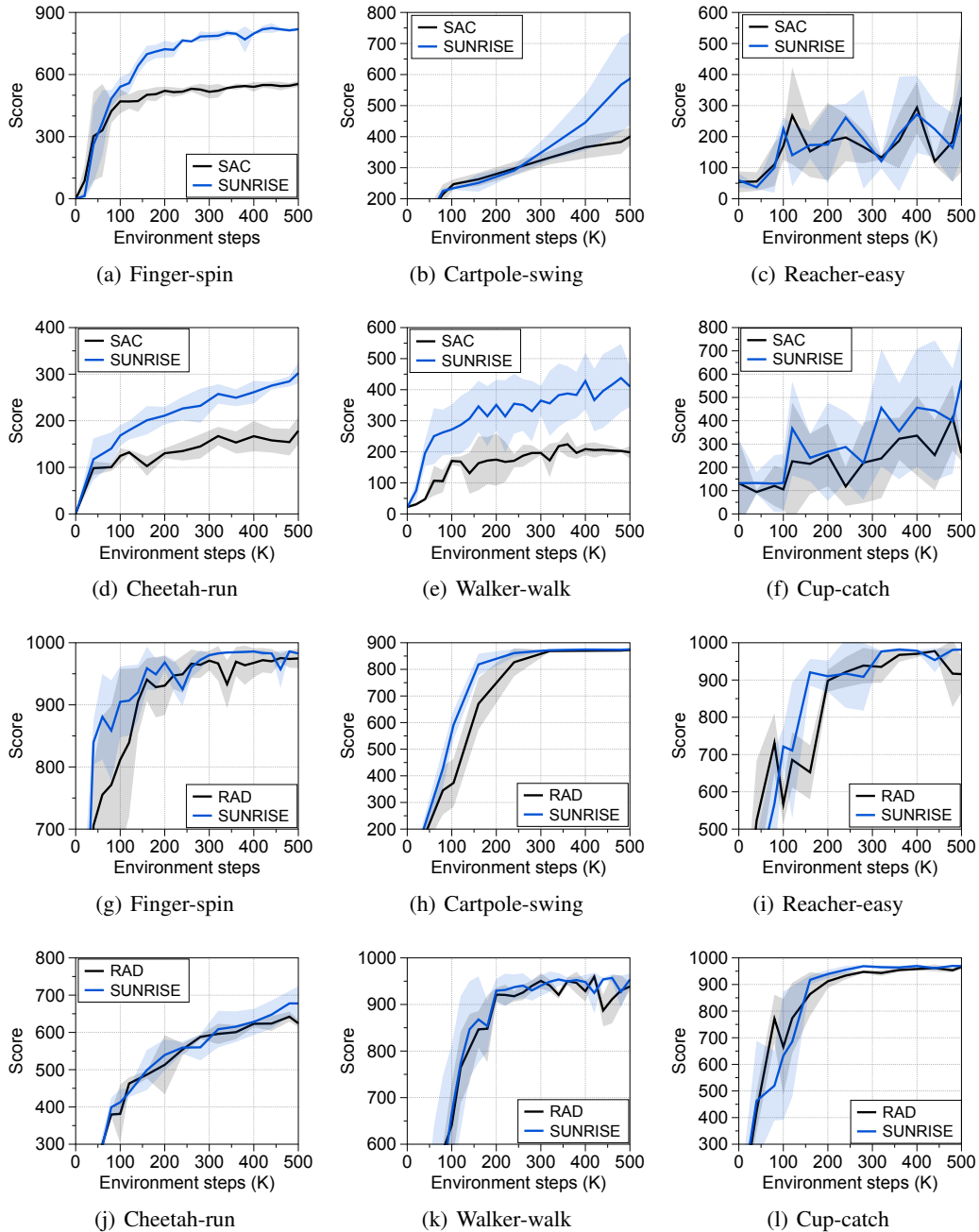


Figure 5: Learning curves of (a-f) SAC and (g-l) RAD on DeepMind Control Suite. The solid line and shaded regions represent the mean and standard deviation, respectively, across five runs.

F Experimental setups and results: Atari games

Training details. We consider a combination of sample-efficient versions of Rainbow DQN and SUNRISE using the publicly released implementation repository (<https://github.com/Kaixhin/Rainbow>) without any modifications on hyperparameters and architectures. For our method, the temperature for weighted Bellman backups is chosen from $T \in \{10, 40\}$, the mean of the Bernoulli distribution is chosen from $\beta \in \{0.5, 1.0\}$, the penalty parameter is chosen from $\lambda \in \{1, 10\}$, and we train five ensemble agents. The optimal parameters are chosen to achieve the best performance on training environments. Here, we remark that training ensemble agents using same training samples but with different initialization (i.e., $\beta = 1$) usually achieves the best performance in most cases similar to Osband et al. [33] and Chen et al. [10]. We expect that this is because splitting samples can reduce the sample-efficiency. Also, initial diversity from random initialization can be enough because each Q-function has a unique target Q-function, i.e., target value is also different according to initialization.

Learning curves. Figure 6, Figure 7 and Figure 8 show the learning curves on all environments.

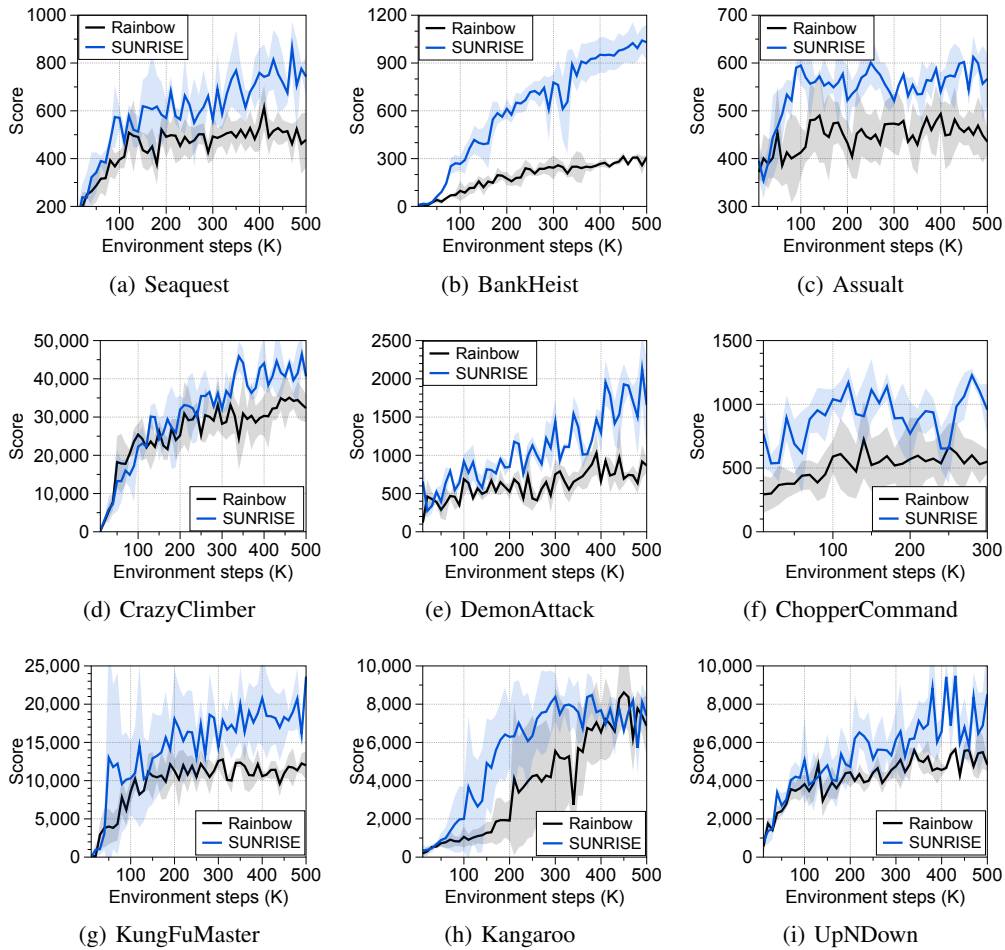


Figure 6: Learning curves on Atari games. The solid line and shaded regions represent the mean and standard deviation, respectively, across three runs.

G Experimental setups and results: stochastic reward OpenAi Gym

DisCor. DisCor [27] was proposed to prevent the error propagation issue in Q-learning. In addition to a standard Q-learning, DisCor trains an error model $\Delta_\psi(s, a)$, which approximates the cumulative

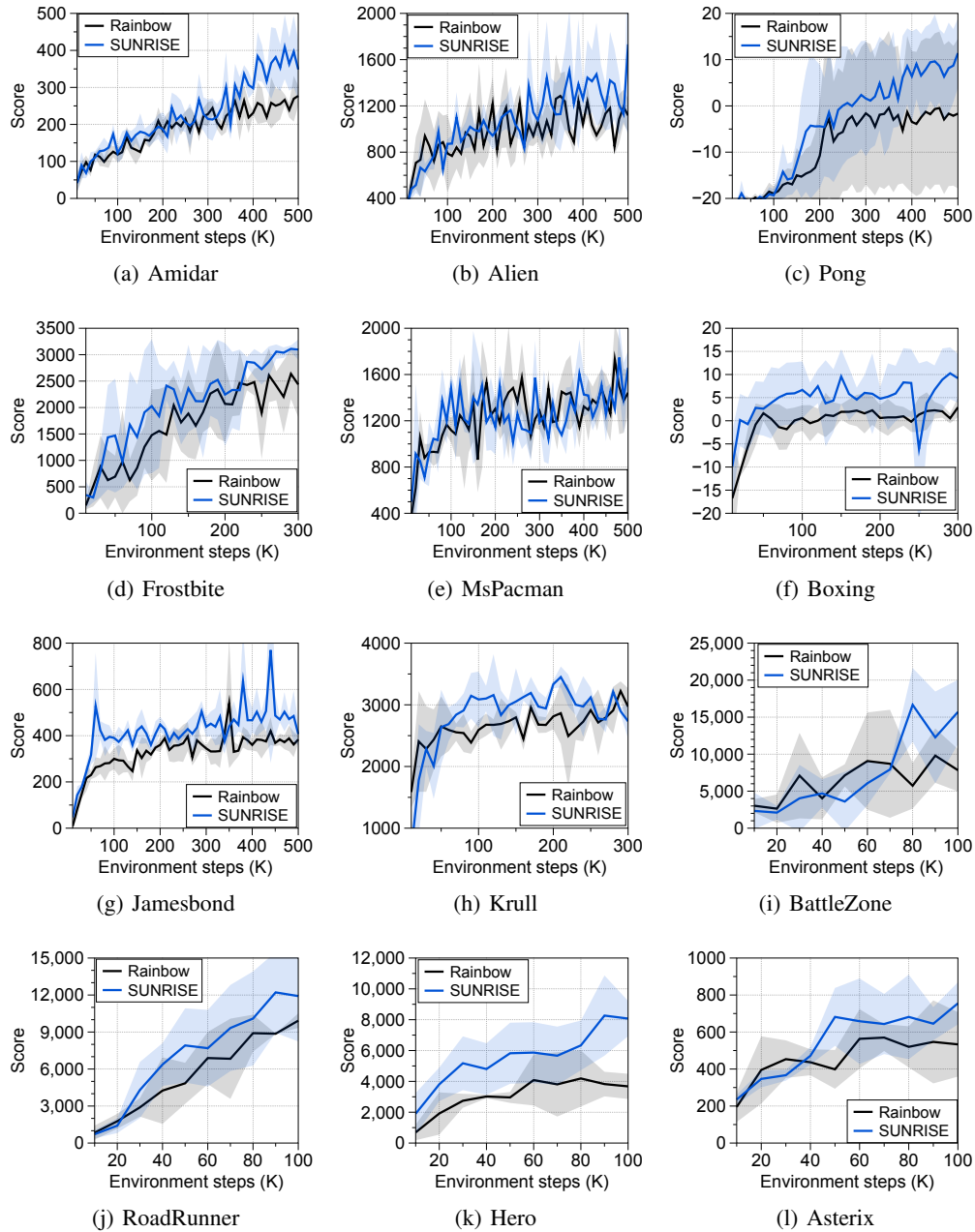


Figure 7: Learning curves on Atari games. The solid line and shaded regions represent the mean and standard deviation, respectively, across three runs.

sum of discounted Bellman errors over the past iterations of training. Then, using the error model, DisCor reweights the Bellman backups based on a confidence weight defined as follows:

$$w(s, a) \propto \exp\left(-\frac{\gamma \Delta_{\psi}(s, a)}{T}\right),$$

where γ is a discount factor and T is a temperature. By following the setups in Kumar et al. [27], we take a network with 1 extra hidden layer than the corresponding Q-network as an error model, and chose $T = 10$ for all experiments. We update the temperature via a moving average and use the learning rate of 0.0003. We use the SAC algorithm as the RL objective coupled with DisCor and

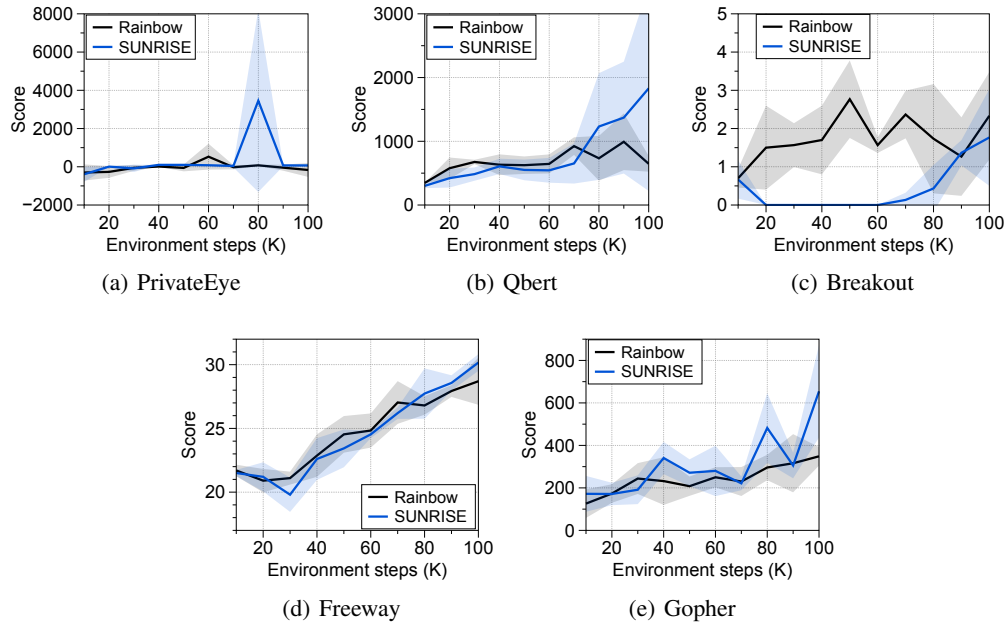


Figure 8: Learning curves on Atari games. The solid line and shaded regions represent the mean and standard deviation, respectively, across three runs.

build on top of the publicly released implementation repository (<https://github.com/vitchyr/rlkit>).

Learning curves. Figure 9 shows the learning curves of SUNRISE and DisCor on stochastic reward OpenAi Gym environments. SUNRISE outperforms baselines such as SAC and DisCor, even when only using the proposed weighted Bellman backup (green curve). This implies that errors in the target Q-function can be characterized by the proposed confident weight in (5) effectively. By additionally utilizing UCB exploration, both sample-efficiency and asymptotic performance of SUNRISE are further improved (blue curve).

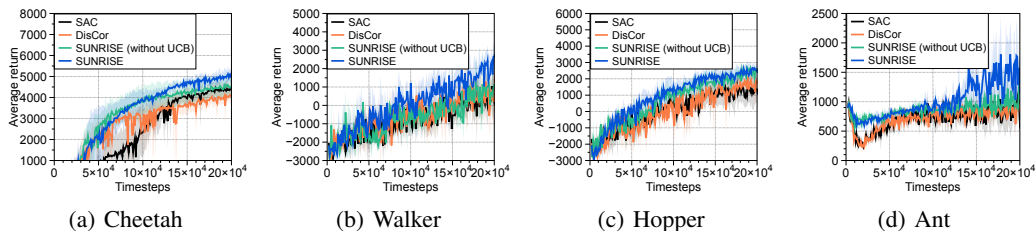


Figure 9: Comparison with DisCor on (a) Cheetah, (b) Walker, (c) Hopper, and (d) Ant environments with stochastic rewards. We add Gaussian noises to reward function to increase an error in value estimations.